Soil-water characteristic curve of polypropylene fibre-reinforced sandy soil

Cíntia Lopes de Castro[1]# (iD), Anderson Borghetti Soares[1] (iD),

Marcos Fábio Porto de Aguiar[2] (iD)

Article

Abstract

Fibre reinforcement is considered a good alternative for improving the geotechnical properties of soil. However, studies that investigate its behaviour, accounting for the unsaturated condition, and the hydraulic behaviour of soil mixtures with fibre, are limited. Therefore, the current study evaluates the impact of the inclusion of polypropylene fibres on the hydraulic behaviour of soil through geotechnical characterisation, scanning electron microscopy (SEM), macroporosity and microporosity tests, and filter paper tests. The soil-water characteristic curve (SWCC) of different mixtures of fibre-reinforced soil was adjusted by the models enshrined in the literature, using polypropylene fibres of length 6 mm, diameter 18 μm, and fibre contents 0.25% (SF025), 0.75% (SF075), 1.0% (SF100), and 1.25% (SF125) relative to the dry weight of the soil. The results indicated a transition from unimodal to bimodal shape in the SWCC for the polypropylene fibre-reinforcement, suggesting that their inclusion altered the soil structure. The same bimodal behaviour of SWCC was observed in all reinforced samples that produced similar values of air-entry suction and residual volumetric water content, but with increased water retention for the same level of suction for higher fibre content. The results of the tension table test indicated an increase in the volume of macropores with an increase in fibre content and a decrease in micropore volumes. These results agree with the compaction tests, which showed a decrease in the dry maximum density with an increased fibre content, whereas the optimum water content increased.

1. Introduction

Applying polypropylene fibres to layers of soil in geotechnical projects, such as landfills on soft soils, slopes, and covers for sanitary landfills or surface foundations, improve the mechanical behaviour of these structures, particularly through increased strength, ductility, and tenacity, and in limiting post-peak reduction in resistance (Al-Refeai, 1991; Consoli et al., 2009; Yilmaz, 2009; Falorca & Pinto, 2011; Olgun, 2013; Chen et al., 2015; Festugato et al., 2017; Mirzababaei et al., 2018).

Fibre-reinforced soils are subjected to variations in moisture on site, often in their unsaturated state. However, studies investigating the hydromechanical behaviour of fibre-reinforced soils under unsaturated conditions are limited (Al-Mahbashi et al., 2020). Therefore, the study of this condition is important and necessary to understand the behaviour to determine their geotechnical properties.

The soil-water characteristic curve (SWCC), also referred to as the retention curve, is a key property for implementing unsaturated soil mechanics in engineering practice. The SWCC is a measure of the variations in the water storage capacity within the macropores and micropores of the soil undergoing matric suction variation (Fredlund et al., 2012). Malekzadeh & Bilsel (2014) investigated the effects of including polypropylene fibres in the SWCC of expansive soil. The results showed that fibre-reinforcement increased the adhesion between soil particles and the air-entry suction values.

Several in situ and laboratory techniques can be used to measure the suction. Different suction measurement techniques have been employed by Southen & Kerry Rowe (2007), Miguel & Bonder (2012), and Priono et al. (2016). Among them, the filter paper technique has been widely used to obtain the SWCC of porous materials because suction measurements can be easily performed at a low cost, and a wide suction interval can be measured (Leong et al., 2002).

Castro et al., Soil. Rocks, São Paulo, 2022 45(3):e2022070021

1

The filter paper test is performed by placing the soil in contact with a filter paper that can absorb the water in the soil until a certain balance condition is attained, such that the matric potentials of water in the soil and porous material are equal.

SWCC may be influenced by various factors, such as void ratio, soil type, soil structure, particle size distribution, stress state, mineralogy, degree of weathering, and pore size distribution (Yang et al., 2004; Zhou & Jian-lin, 2005; Priono et al., 2016).

Moreover, SWCCs may display unimodal and bimodal shapes (Burger & Shackelford, 2001; Li & Zhang, 2009; Satyanaga et al., 2013; Li et al., 2014, Wijaya & Leong, 2017). Unimodal curves exhibit a single desaturation stretch, whereas bimodal curves display two stretches of desaturation, and consequently exhibit two air-entry values: the first corresponds to a pore family of relatively large pores and the second to another family of small pores (Gitirana Junior & Fredlund, 2004).

Generally, bimodal SWCC is attributed to double porosity in the soil, which may appear as a result of the bimodal distribution of the particle sizes, compaction, or other characteristics such as cracks in the earth (Li & Zhang, 2009; Satyanaga et al., 2013; Li et al., 2014). In soils with double porosity, the pores are largely governed by the layout of coarse and fine particles, resulting in large (macropores) and small pores (micropores), respectively (Burger & Shackelford, 2001).

The SWCC is obtained by adjusting the experimental points using mathematical equations. Many researchers have proposed adjustment models that are valid for certain soil types and suction ranges (Van Genuchten, 1980; Fredlund & Xing 1994; Gitirana Junior & Fredlund, 2004).

Gitirana Junior & Fredlund (2004) proposed a set of equations, which includes the adjustment of bimodal curves with two air-entry values and two residual points. The other models can be adapted to bimodal curves using the equations for two stretches joined by junction suction, that is, considering two unimodal curves. Various equations for adjusting the unimodal and bimodal characteristic curves and for determining the adjustment parameters have been proposed by Satyanaga et al. (2013), Li et al. (2014), Wijaya & Leong (2016), and Leong (2019).

The current study presents the behaviour of the SWCC of polypropylene fibre-reinforced soil, based on the results of an experimental program developed with a mixture of sandy soil with different polypropylene fibre contents, and investigates the influence of the fibres on the hydraulic behaviour of mixtures. Fibre reinforcement in sandy soil can affect the structure of the composite, changing the macro and microporosity, and consequently, the mechanical and hydraulic properties, such as the saturated permeability, unsaturated permeability, and soil-water retention (SWR) curve. These changes in the structure result in different drainage conditions and water retention capacities, which are fundamental to the performance of unsaturated soils, such as landfill waste cover, foundations, and slopes with reinforced soils.

2. Materials and methods

The soil used in the study was collected from the Geotechnics and Foundations Test Field (GECEF), Federal University of Ceará (UFC) in Fortaleza, Ceará State, Northeast Brazil. Disturbed samples were collected at a depth of 10 cm using shovel and picks, and thereafter they were sent to the laboratory and packed in plastic bags in sufficient quantities for reinforcement with fibres, according to NBR 6457 (ABNT, 2016a).

Table 1 presents the results of the geotechnical characterisation of the soil and grading curve, according to NBR 7181 (ABNT, 2016c), ASTM D7928 (ASTM, 2021b), and ASTM D6913 (ASTM, 2017b), as shown in Figure 1. This soil was classified as poorly graded silty sand (SM–SP) according to the Unified Soil Classification System (USCS). The liquid limit, NBR 6459 (ABNT, 2017), plastic limit, NBR 7180 (ABNT, 2016b), and ASTM D4318 (ASTM, 2017a), indicate that the soil has non-plastic (NP) characteristics.

The polypropylene fibre contents analysed were 0% (SN), 0.75% (SF075), 1.0% (SF100), and 1.25% (SF125) of the dry weight of the soil. The polypropylene fibres used in this study consisted of extremely fine filaments produced through an extrusion process. The fibres were of length 6 mm, diameter 18 μm, specific weight 0.91 g/cm^3, tensile

Table 1. Physical properties of soil.

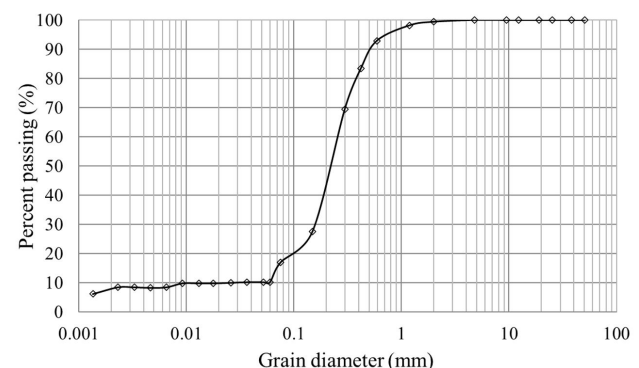| Property	Value
Specific gravity	2.56
Coarse sand (0.6 < diameter < 2 mm)	7.0%
Medium sand (0.2 < diameter < 0.6 mm)	51.0%
Fine sand coefficient (0.06 < diameter < 0.2 mm)	32.0%
Silt (0.002 < diameter < 0.06 mm)	2.0%
Clay (diameter <0.002 mm)	8.0%
Uniformity coefficient (C_u)	28.9
Curvature coefficient (C_c)	12.4

Figure 1. Particle size distribution curve.

shear strength 300 MPa, elastic modulus 3 GPa, and shear elongation of 80%, with a circular section (Figure 2).

2.1 Experimental program

The experimental program included compaction characterisation tests, filter paper tests, scanning electron microscopy (SEM), and macroporosity and microporosity tests.

2.1.1 Sample preparation

To homogenise the material, the dry components of the mixture (soil and fibre) were first manually mixed, after which water was added, and the mixture was visually verified. The compaction test according to NBR 7182 (ABNT, 2020) and ASTM D698 (ASTM, 2021a), with normal Proctor energy, was performed for the natural soil and soil–fibre mixtures, and test samples were moulded using the values obtained for the optimum water content (w) and corresponding maximum dry unit weights ($\gamma_{d, max}$), which are provided in Table 2. Figure 3 shows the compaction curves obtained for the natural soil and soil–fibre mixtures.

The test samples were compacted inside aluminium rings of diameter 5 cm and height 2 cm to attain the density corresponding to the maximum dry apparent specific weight. Figure 3 shows an increase in the optimum water content and a reduction in the maximum dry weight by increasing the fibre content. This behaviour in the compaction curves was observed for mixtures of natural fibre with different soils

by Oliveira Junior (2018) and Ayala (2020), indicating an increase in the porosity of the mixture.

2.1.2 Filter paper technique

The filter paper technique was adopted according to ASTM D 5298 (ASTM, 2016). A Whatman No. 42 filter paper was placed directly from the box over the sample surface. Curves were obtained by drying the samples. After the equalisation period between the filter paper and the seven-day soil, the gravimetric moisture of the filter paper was measured, and the matric suction (Ψ) was obtained from the calibration equations proposed by Chandler et al. (1992), as follows, in Equations 1 and 2:

For filter paper moisture < 47%:

$$\Psi\left(kPa\right) = 10^{4.842 \,-\, 0.0622w} \tag{1}$$

For filter paper moisture > 47%:

$$\Psi\left(kPa\right) = 10^{6.050 \,-\, 2.48\, Logw} \tag{2}$$

The samples were homogenised at the optimal water content and dynamically compacted into three layers in a metallic ring of diameter 5 cm and height 2 cm. The filter paper technique is suitable for suction values between 10–29000 kPa (Marinho, 1994).

Table 2. Parameters of compaction curves.

Sample	w (%)	$\gamma_{d, max}$ (kN/m³)
N	9.6	19.09
SF025	10.5	18.60
SF075	10.6	18.31
SF100	11.3	18.18
SF125	11.5	17.95

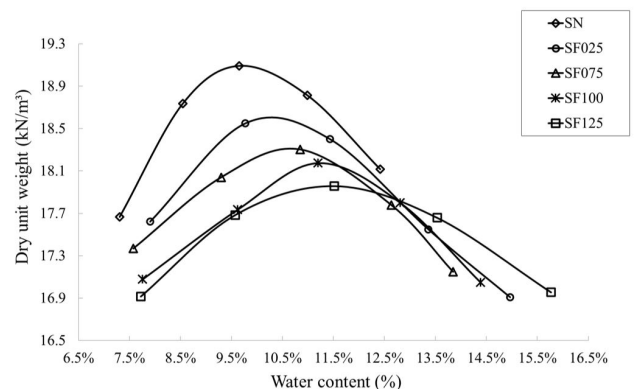**Figure 2.** Polypropylene fibres.

Figure 3. Compaction curves.

2.1.3 Soil-water characteristic curve functions

The models proposed by Fredlund & Xing (1994) and Gitirana Junior & Fredlund (2004) (hereafter referred to as FX and GF, respectively) were applied to obtain the adjusted SWCC using the experimental points obtained from the filter paper technique. The equation proposed by Fredlund & Xing (1994) was applied to unimodal SWCCs; however, bimodal SWCCs can be obtained by adaptation, considering the equation applied to two unimodal curves connected by junction suction. Gitirana Junior & Fredlund (2004) proposed an equation for bimodal SWCCs defined by two air-entry values and two residual points, resulting in four curve inflection points.

2.1.4 SEM

SEM was used to visualise the soil structure and analyse the shape, distribution, soil–fibre adhesion, and connection between the voids inside the tested samples. Pictures of the samples were enlarged to 120 times their actual size. The samples under analysis were first compacted in a ring of diameter 5 cm and height 2 mm, and dried in an oven at 105 °C.

2.1.5 Macro and microporosity testing

The macroporosity and microporosity of the soil samples were determined using a stress table (EMBRAPA, 1997), which is fast, simple, easy to use, and common in agricultural sciences.

In this method, a stress corresponding to a 60 cm high water column, that is, 6 kPa, is applied to the saturated samples, which would cause the water to drain from the macropores. The application of a tension of 6 kPa in sandy soils is sufficient to drain water in the macropores and retain the water in the micropores (Teixeira et al., 2017). After drainage, the samples were oven-dried at 105 °C, and the micropore percentage was determined, corresponding to the remaining water in the soil. The difference between the saturated water percentage (total porosity) and the micropore percentage provides the macropore percentage, as the total porosity is the sum of the macropore and micropore percentages of the soil sample.

3. Analysis and results

3.1 Soil-water characteristic curve

The SWCC obtained by drying the natural soil and soil–fibre mixtures was expressed in terms of suction and volumetric water content. Figure 4 shows the experimental filter paper test results for the natural soil sample and soil–fibre mixtures. The experimental points obtained from the filter paper method for natural soil were observed to tend toward unimodal behaviour, whereas the soil–fibre samples

exhibit a bimodal shape in the SWCC, suggesting that the macrostructure and microstructure of the soil were affected by the inclusion of fibres, resulting in a change in the hydraulic behaviour of the samples.

The SWCCs were adjusted using the FX and GF methods. Figure 5 shows SWCC for the natural soil. The adjustments by both methods used were approximate, indicating that the air-entry suction value was less than 1 kPa and the residual volumetric water content was approximately 2.5%. These values are typical of sandy soils, and agree with the results reported by Fredlund & Xing (1994).

Figures 6 to 9 show the SWCC of the fibre-reinforced soil for the analysed fibre contents (0.25%, 0.75%, 1.0%, and 1.25%, respectively) adjusted by the FX and GF methods. Although a marginal dispersion of the experimental data was identified, the models were adequate, because it was possible to identify the shape of the SWCCs.

Tables 3 and 4 show the parameters adopted for the mathematical adjustment using the equations proposed by Fredlund & Xing (1994) and Gitirana Junior & Fredlund (2004) describing the unimodal SWCCs of the natural soil and bimodal SWCCs of the soil–fibre mixtures. The results revealed that the SWCCs behaved similarly and agreed significantly with the behaviour of the experimental points obtained from the filter paper test. A significant aspect of the
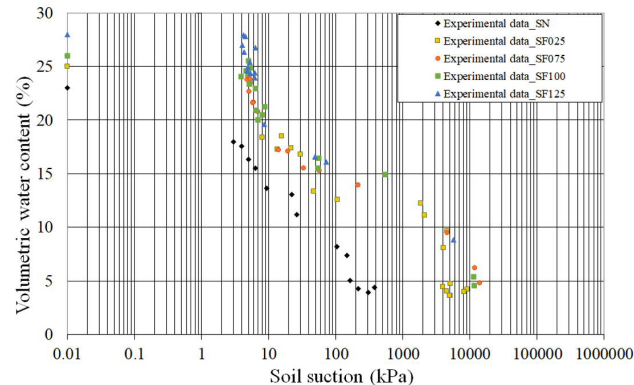

Figure 4. Experimental points obtained from the filter paper test on natural soil and soil–fibre mixture.
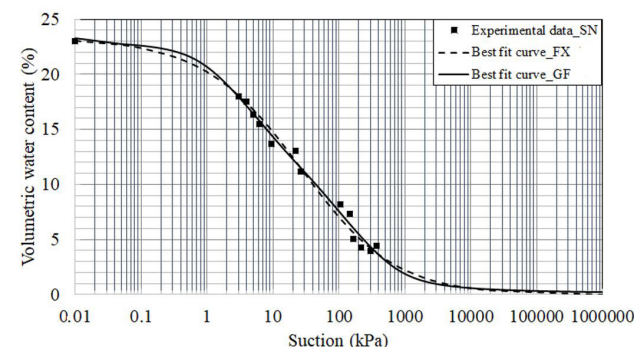

Figure 5. SWCC-natural soil.

Castro et al.

SWCC analysis is the change in the curve behaviour from unimodal to bimodal shape when the soil is reinforced with polypropylene fibres, suggesting that the macrostructure and microstructure of the soil were affected by the fibre inclusion. The bimodal behaviour of SWCC was observed by Abdallah et al. (2019) in sandy soil (with fines) and lint wool residues.

The analysis of the water retention curves revealed that an increase in the volumetric water content was observed for the same suction with an increase in the fibre content (Figure 10). This behaviour was also observed in fibre–soil mixtures with clayey and sandy soils and natural and synthetic fibres (Saad, 2016; Gusmão, 2020; Gusmão & Jucá, 2021; Abdallah et al., 2019; Ayala, 2020).

3.2 SEM

Figure 11 shows the micrograph results of the compacted samples of the natural soil (Figure 10a) and
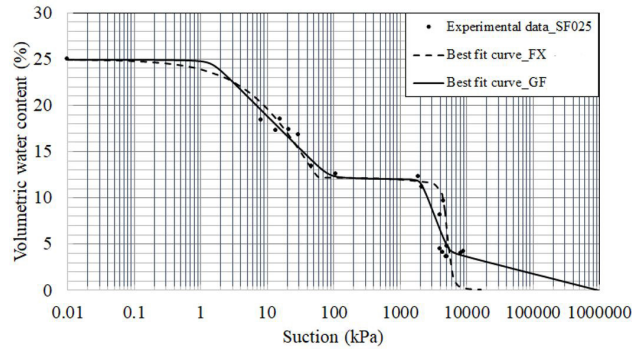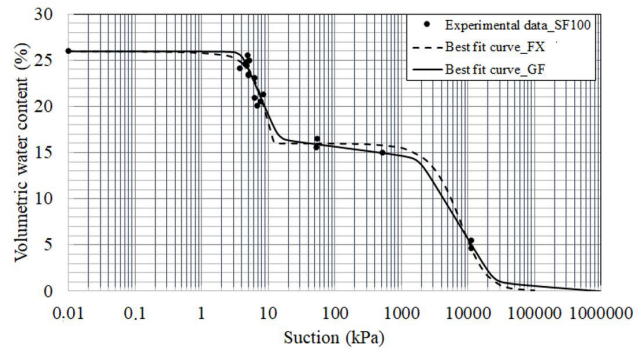

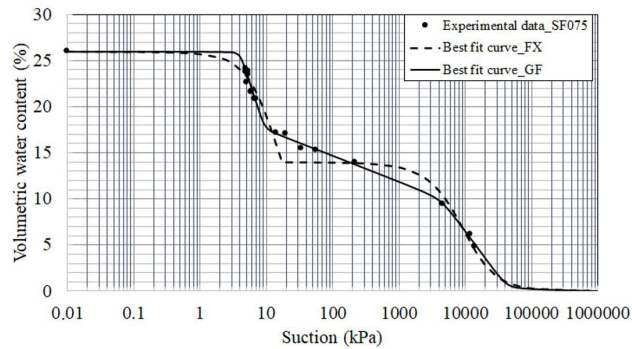**Figure 6.** SWCC-SF025.

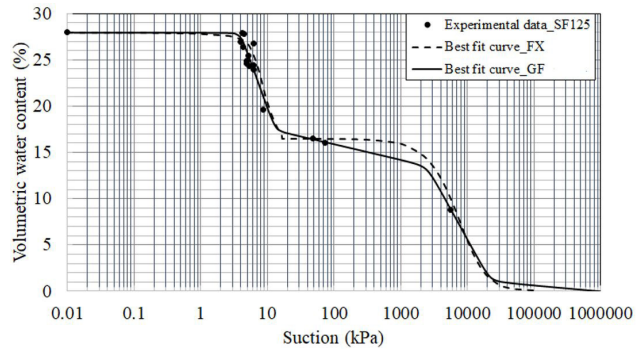**Figure 8.** SWCC-F100.

Figure 7. SWCC-SF075.

Figure 9. SWCC-SF125.

Table 3. Adjustment parameters of the equation proposed by Fredlund & Xing (1994) for the behaviour of the soil–fibre samples.

Sample	Macropores				Micropores			
	a (kPa)	n	m	Ψ_r (kPa)	a'	n'	m'	$\Psi_{r'}$ (kPa)
SN	29	0.56	2.7	1100	--	--	--	--
SF025	31	0.78	1.68	50	5000	12.1	1.97	11800
SF075	9.5	2.19	0.87	15	10000	1.9	3.62	30000
SF100	7.2	3.68	0.51	12	10000	1.77	3.6	30000
SF125	6.4	6.27	0.25	16.5	10000	1.72	3.71	30000

Table 4. Adjustment parameters of the equation proposed by Gitirana Junior & Fredlund (2004) for the behaviour of the soil–fibre samples.

Sample	Ψ_{b1} (kPa)	Ψ_{r1} (kPa)	θ_{r1} (%)	Ψ_{b2} (kPa)	θ_b (%)	Ψ_{r2} (kPa)	θ_{r2} (%)	a
SN	1.6	670	0.025	--	--	--	--	0.093
SF025	1.45	84.43	12.1	2031.7	12.1	5293.4	4.15	0.020
SF075	4	9.319	17.52	4410.6	10.2	42275	0.26	0.022
SF100	4	14.19	16.41	1836.4	14.56	24740.2	0.88	0.022
SF125	4	13.06	17.4	2506.6	13.6	21993.3	1.04	0.020

Castro et al., Soil. Rocks, São Paulo, 2022 45(3):e2022070021

soil–fibre mixtures (Figure 10b–10d). The morphological characteristics indicating the texture, structure, and adhesion between materials can be observed.

The micrograph of natural soil illustrates the presence of voids and irregularly shaped particles. In the micrograph of the soil–fibre mixtures, soil clusters were predominant, causing apparently larger voids compared to those formed in the natural soil. The fibre agglomerations hinder the connection and interlocking between the soil particles, and little adhesion of the materials is observed.

Moreover, the polypropylene fibres disposed in random directions interfere with the continuity of the pores, thereby increasing the desaturation path and the capacity to retain
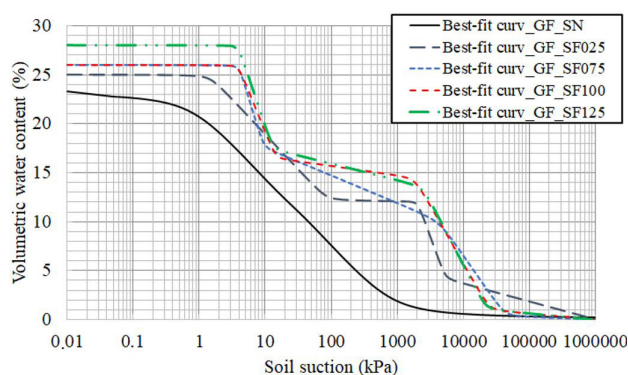
macropores. These characteristics justify the increased total porosity of the soil–fibre mixtures and confirm the change in the soil structure, causing an alteration in the shape of the SWCC. In all cases, agglomeration of fibres with large voids was verified, which may explain the macroporosity observed in the tests.

3.3 Analysis of macroporosity and microporosity

Macroporosity and microporosity were determined using the stress table method to investigate the relationship between the macropores and micropores of the reinforced samples. Figure 12 shows the test results as percentages of macropores and micropores. The microporosity percentage was significantly higher (approximately 80%) than the macroporosity percentage (approximately 20%). This result was expected, because the amount of added fibre was relatively small compared to that of soil in the sample. These results agree with the compaction curves, which show that increasing the fibre content in the mixture decreased the maximum apparent specific weight and increased the optimal water content.

In addition, the soil was predominantly composed of medium to fine sand, as confirmed in the particle size analysis, thus possibly resulting in the formation of a larger number of small voids, that is, micropores. A sharp increase in macroporosity was observed with the increase in fibre
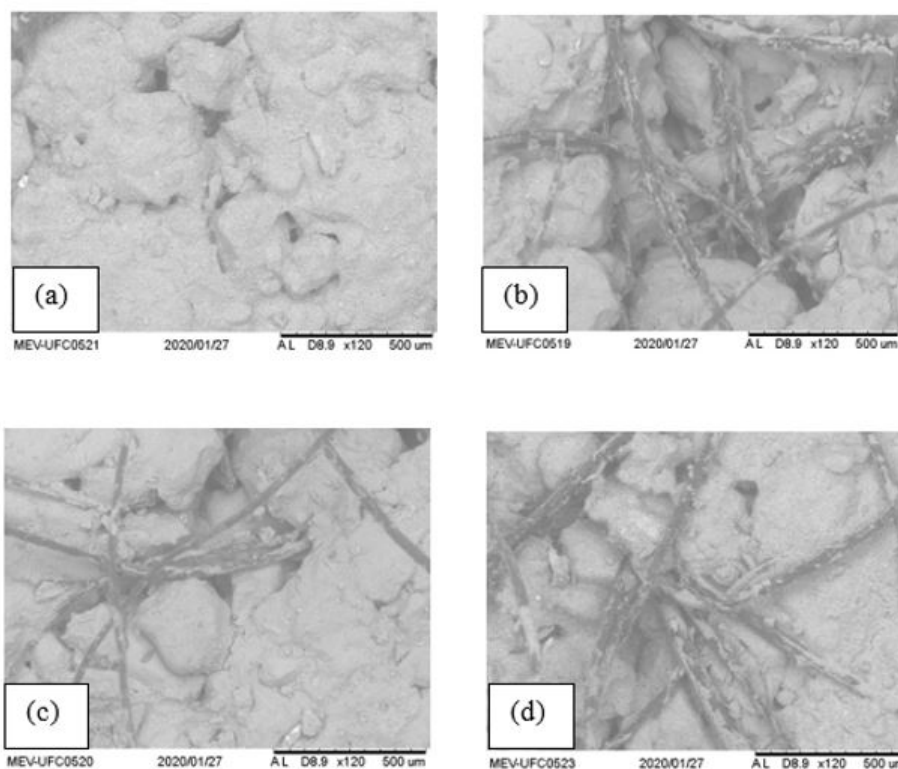

Figure 10. SWR curves with different fibre contents.

Figure 11. SEM micrograph results (× 120): (a) natural soil; soil–fibre mixtures: (b) SF075, (c) SF100 (d) SF125.
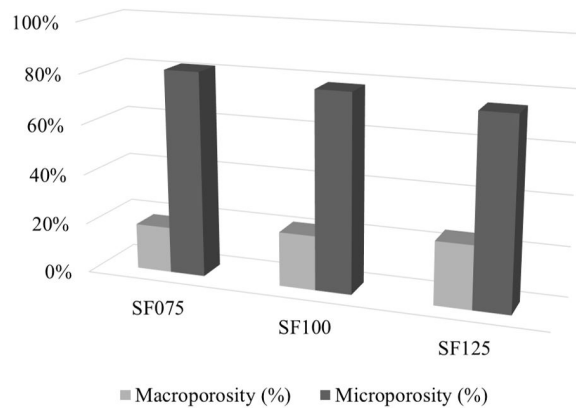
Figure 12. Results of the macroporosity and microporosity test.

content, as expected, because the increase in fibre content resulted in the increase of the porosity of the mixture.

4. Conclusion

The geotechnical properties of soil–fibre mixtures are important in geotechnical engineering. Therefore, determining the physical properties of the composites is necessary. The inclusion of fibre in the soil can affect the soil structure and the hydromechanical properties of the composite. This study aimed to evaluate the effect of the addition of propylene fibre to sandy soils on the SWCCs.

The compaction curves showed that the inclusion of propylene fibre resulted in a decrease in the maximum dry weight and an increase in the optimum water content, indicating an increase in the soil porosity. Through SEM, a considerable quantity of voids and irregularity in the shape of the soil particles could be identified. The soil–fibre samples demonstrated a predominance of soil and fibre agglomerations, with apparently larger voids compared to the natural soil. At the soil–fibre interface, a significant number of voids and regions with little adhesion to the materials were apparent, with the formation of fibre clusters that hinder the connection and interlocking between the soil particles and fibres. The results of the macroporosity and microporosity tests using the stress table indicated that the increase in the fibre content in the soil increased the macroporosity of the reinforced samples.

The SWCCs of the natural soil and the soil–polypropylene fibre mixtures were derived from the experimental points obtained through the filter paper technique, and adjusted by the GF method, as it was closer to the experimental points obtained. The results showed that when the soil was reinforced with fibres, the SWCC changed from unimodal to bimodal shape for the fibre contents studied, suggesting that the macrostructure and microstructure of the soil were influenced by the inclusion of fibres, which consequently influenced the hydromechanical behaviour of the soil. Furthermore, an increase in volumetric water content was observed for the

same suction with an increase in fibre content. The results of this study are limited to the SWCC and structure of propylene fibre–soil mixtures, and further research is required to study the complete hydraulic parameters, such as unsaturated and saturated permeabilities, and mixtures with different types of soils and fibres.

Acknowledgements

Declaration of interest

The authors declare that there are no conflicts of interest regarding the publication of this paper.

Authors' contributions

Cíntia Lopes de Castro: conceptualisation, methodology, validation, writing - original draft. Anderson Borghetti Soares: supervision, validation, writing - review & editing. Marcos Fábio Porto de Aguiar: supervision, validation, writing—review & editing.

List of symbols

a, a'	SWCC adjustment parameter;
m, m'	SWCC adjustment parameter;
n, n'	SWCC adjustment parameter;
SWCC	Soil-water characteristic curve;
w	Optimum water content;
$\gamma_{d, max}$	Maximum dry specific weight;
θ	Volumetric water content
θ_b	Volumetric water content at air-entry value;
θ_r	Volumetric water content in residual state;
θ_{r1}	First volumetric water content in residual state
θ_{r2}	Second volumetric water content in residual state.
Ψ	Matric suction;
Ψ_b	Air-entry value;
Ψ_{b1}	First air-entry value
Ψ_{b2}	Second air-entry value
Ψ_r	Residual state of air-entry value;
Ψ_{r1}	Residual state of first of air-entry value
Ψ_{r2}	Residual state of second air-entry value

References

Abdallah, A., Ugolini, F., Baronti, S., Maienza, A., Camilli, F., Bonora, L., Marteli, F., Primicerio, J., & Ungaro, F. (2019). Potential of recycling wool residues as an

amendment for enhancing the physical and hydraulic properties of sandy loam soil. *International Journal of Recycling of Organic Waste in Agriculture*, 8(Suppl. 1), 131-143. http://dx.doi.org/10.1007/s40093-019-0283-5.

ABNT NBR 6457. (2016a). *Soil samples - Preparation for compaction and characterization tests*. ABNT - Associação Brasileira de Normas Técnicas, Rio de Janeiro, RJ (in Portuguese).

ABNT NBR 7180. (2016b). *Soil - Plasticity limit determination*. ABNT - Associação Brasileira de Normas Técnicas, Rio de Janeiro, RJ (in Portuguese).

ABNT NBR 7181. (2016c). *Soil - Grain size analysis*. ABNT - Associação Brasileira de Normas Técnicas, Rio de Janeiro, RJ (in Portuguese).

ABNT NBR 6459. (2017). *Soil - Liquid limit determination*. ABNT - Associação Brasileira de Normas Técnicas, Rio de Janeiro, RJ (in Portuguese).

ABNT NBR 7182. (2020). *Soil - Compaction test*. ABNT - Associação Brasileira de Normas Técnicas, Rio de Janeiro, RJ (in Portuguese).

Al-Mahbashi, A.M., Al-Shamrani, M.A., & Moghal, A.A.B. (2020). Soil–water characteristic curve and one-dimensional deformation characteristics of fiber-reinforced lime-blended expansive soil. *Journal of Materials in Civil Engineering*, 32(6), 04020125-1-04020125-9. https://doi.org/10.1061/(ASCE)MT.1943-5533.0003204.

Al-Refeai, T.O. (1991). Behavior of granular soils reinforced with discrete randomly oriented inclusions. *Geotextiles and Geomembranes*, 10(4), 319-333. http://dx.doi.org/10.1016/0266-1144(91)90009-L.

ASTM D5298-03. (2016). *Standard Test Method for Measurement of Soil Potential (Suction) Using Filter Paper*. ASTM International, West Conshohocken, PA.

ASTM D4318. (2017a). *Standard Test Methods for Liquid limit, Plastic limit and Plastic Index of soils*. ASTM International, West Conshohocken, PA.

ASTM D6913. (2017b). *Standard Test Methods for Particle-size Distribution (Gradation) of Soils Using the Sieve Analysis*. ASTM International, West Conshohocken, PA.

ASTM D698:12. (2021a). *Standard Test Methods for Laboratory Compaction Characteristics of Soils using Standard Effort*. ASTM International, West Conshohocken, PA.

ASTM D7928. (2021b). *Standard Test Methods for Particle-size Distribution of Fine-Grained soils using the sedimentation analysis*. ASTM International, West Conshohocken, PA.

Ayala, R.J.L. (2020). *Melhoria de Solos com Fibras Provenientes da Indústria Avícola* [Doctoral thesis]. Departamento de Engenharia Civil e Ambiental, Universidade de Brasília.

Burger, C.A., & Shackelford, C.D. (2001). Soil-water characteristic curves and dual porosity of sand–diatomaceous earth mixtures. *Journal of Geotechnical and Geoenvironmental Engineering*, 127(9), 790-800. http://dx.doi.org/10.1061/(ASCE)1090-0241(2001)127:9(790).

Chandler, R.J., Crilly, M.S., & Montgomery-Smith, G. (1992). A low cost method of assessing clay desiccation for low-rise buildings. *Proceedings of the Institution of Civil Engineers. Civil Engineering*, 92(2), 82-89. http://dx.doi.org/10.1680/icien.1992.18771.

Chen, M., Shen, S.L., Arulrajah, A., Wu, H.N., Hou, D.W., & Xu, Y.S. (2015). Laboratory evaluation on the effectiveness of polypropylene fibers on the strength of fiber-reinforced and cement-stabilized Shanghai soft clay. *Geotextiles and Geomembranes*, 43(6), 515-523. http://dx.doi.org/10.1016/j.geotexmem.2015.05.004.

Consoli, N.C., Festugato, L., & Heineck, K.S. (2009). Strain-hardening behaviour of fibre-reinforced sand in view of filament geometry. *Geosynthetics International*, 16(2), 109-115. http://dx.doi.org/10.1680/gein.2009.16.2.109.

Empresa Brasileira de Pesquisa Agropecuária – EMBRAPA. (1997). *Manual de métodos de análise de solos* (2. ed., 212 p). Rio de Janeiro/RJ: Embrapa Solos.

Falorca, I.M.C.F.G., & Pinto, M.I.M. (2011). Effect of short, randomly distributed polypropylene microfibres on shear strength behaviour of soils. *Geosynthetics International*, 18(1), 2-11. http://dx.doi.org/10.1680/gein.2011.18.1.2.

Festugato, L., Menger, E., Benezra, F., Kipper, E.A., & Consoli, N.C. (2017). Fibre-reinforced cemented soils compressive and tensile strength assessment as a function of filament length. *Geotextiles and Geomembranes*, 45(1), 77-82. http://dx.doi.org/10.1016/j.geotexmem.2016.09.001.

Fredlund, D.G., & Xing, A. (1994). Equations for the soil-water characteristic curve. *Canadian Geotechnical Journal*, 31(4), 521-532. http://dx.doi.org/10.1139/t94-061.

Fredlund, D.G., Rahardjo, H., & Fredlund, M.D. (2012). *Unsaturated soil mechanics in engineering practice* (926 p.). New Jersey: John Wiley and Sons.

Gitirana Junior, G.F.N., & Fredlund, D.G. (2004). Soil-water characteristic curve equation with independent properties. *Journal of Geotechnical and Geoenvironmental Engineering*, 130(2), 209-211. http://dx.doi.org/10.1061/(ASCE)1090-0241(2004)130:2(209).

Gusmão, L.R.C. (2020). *Influência de ciclos secagem-molhagem no comportamento hidráulico-mecânico de misturas compactadas de solo argiloso com fibras de coco verde* [Master's dissertation]. Programa de Pós-Graduação em Engenharia Civil , Universidade Federal de Pernambuco.

Gusmão, L.R.C., & Jucá, J.F.T. (2021). Influence of green's coconut fiber in unsaturated behavior of compacted clayey soil. *MATEC Web of Conferences*, 337, 01017. https://doi.org/10.1051/matecconf/202133701017.

Leong, E.C. (2019). Soil-water characteristic curves – Determination, estimation and application. *Japanese Geotechnical Society Special Publication*, 7(2), 21-30. http://dx.doi.org/10.3208/jgssp.v07.003.

Leong, E.C., He, L., & Rahardjo, H. (2002). Factors affecting the filter paper method for total and matric suction

measurements. *Geotechnical Testing Journal*, 25(3), 321-332. http://dx.doi.org/10.1520/GTJ11094J.

Li, X., & Zhang, L.M. (2009). Characterization of dual-structure pore-size distribution of soil. *Canadian Geotechnical Journal*, 46(2), 129-141. http://dx.doi.org/10.1139/T08-110.

Li, X., Li, J.H., & Zhang, L.M. (2014). Predicting bimodal soil-water characteristic curves and permeability functions using physically based parameters. *Computers and Geotechnics*, 57, 85-96. http://dx.doi.org/10.1016/j.compgeo.2014.01.004.

Malekzadeh, M., & Bilsel, H. (2014). Hydro-mechanical behavior of polypropylene fiber reinforced expansive soils. *KSCE Journal of Civil Engineering*, 18(7), 2028-2033. http://dx.doi.org/10.1007/s12205-014-0389-2.

Marinho, F.A.M. (1994). Suction measurements with the filter paper method. In *Anais do X Congresso Brasileiro de Mecânica dos Solos e Engenharia de Fundações* (pp. 515-522). Fox do Iguaçu.

Miguel, M.G., & Bonder, B.H. (2012). Soil-water characteristic curves obtained for a colluvial and lateritic soil profile considering the macro and micro porosity. *Geotechnical and Geological Engineering*, 30(6), 1405-1420. http://dx.doi.org/10.1007/s10706-012-9545-y.

Mirzababaei, M., Arulrajah, A., Haque, A., Nimbalkar, S., & Mohajerani, A. (2018). Effect of fiber reinforcement on shear strength and void ratio of soft clay. *Geosynthetics International*, 25(4), 471-480. http://dx.doi.org/10.1680/jgein.18.00023.

Olgun, M. (2013). Effects of polypropylene fiber inclusion on the strength and volume change characteristics of cement-fly ash stabilized clay soil. *Geosynthetics International*, 20(4), 263-275. http://dx.doi.org/10.1680/gein.13.00016.

Oliveira Júnior, A.I. (2018). *Comportamento geotécnico de misturas compactadas de solo argiloso com fibras curtas de coco* [Master's dissertation]. Programa de Pós-Graduação em Engenharia Civil, Universidade Federal de Pernambuco.

Priono, Rahardjo, H., Chatterjea, K., Leong, E.C., & Wang, J.Y. (2016). Effect of hydraulic anisotropy on soil-water characteristic curve. *Soil and Foundation*, 56(2), 228-239. http://dx.doi.org/10.1016/j.sandf.2016.02.006.

Saad, S.S.E. (2016). *Mechanical behavior of fibre reinforced unsaturated clay* [Doctoral thesis] University of Bradford, England.

Satyanaga, A., Rahardjo, H., Leong, E.C., & Wang, J. (2013). Water characteristic curve of soil with bimodal grain-size distribution. *Computers and Geotechnics*, 48, 51-61. http://dx.doi.org/10.1016/j.compgeo.2012.09.008.

Southen, J.M., & Kerry Rowe, R. (2007). Evaluation of the water retention curve for geosynthetic clay liners. *Geotextiles and Geomembranes*, 25(1), 2-9. http://dx.doi.org/10.1016/j.geotexmem.2006.10.002.

Teixeira, P.C., Donagemma, G.K., Fontana, A., & Teixeira, W.G. (2017). *Manual de métodos de análises de solos* (3. ed., 574 p.). Brasília: Empresa Brasileira de Pesquisa Agropecuária, Centro Nacional de Pesquisa de Solos, Ministério da Agricultura e do Abastecimento.

Van Genuchten, M.T. (1980). A closed-form equation for predicting the hydraulic conductivity of unsaturated soils. *Soil Science Society of America Journal*, 44(5), 892-898. http://dx.doi.org/10.2136/sssaj1980.03615995004400050002x.

Wijaya, M., & Leong, E.C. (2016). Equation for unimodal and bimodal soil-water characteristic curves. *Soil and Foundation*, 56(2), 291-300. http://dx.doi.org/10.1016/j.sandf.2016.02.011.

Wijaya, M., & Leong, E.C. (2017). Modelling the effect of density on the unimodal soil-water characteristic curve. *Geotechnique*, 67(7), 637-645. http://dx.doi.org/10.1680/jgeot.15.P.270.

Yang, H., Rahardjo, H., Leong, E.C., & Fredlund, D.G. (2004). Factors affecting drying and wetting soil-water characteristic curves of sandy soils. *Canadian Geotechnical Journal*, 41(5), 908-920. http://dx.doi.org/10.1139/t04-042.

Yilmaz, Y. (2009). Experimental investigation of the strength properties of sand-clay mixtures reinforced with randomly distributed discrete polypropylene fibers. *Geosynthetics International*, 16(5), 354-363. http://dx.doi.org/10.1680/gein.2009.16.5.354.

Zhou, J., & Jian-lin, Y. (2005). Influences affecting the soil-water characteristic curve. *Journal of Zhejiang University. Science*, 6A(8), 797-804. http://dx.doi.org/10.1631/jzus.2005.A0797.